Check for updates

Received: 12 March 2024 | Revised: 17 June 2024 | Accepted: 3 July 2024

DOI: 10.1002/app.56028

RESEARCH ARTICLE

Journal of Applied Polymer Science WILEY

Influence of monomer structure and catalyst concentration on topological transition and dynamic properties of dicarboxylic acid-epoxy vitrimers

Shouqi Shen[1] | **Vijay K. Thakur**[2] | **Alexandros A. Skordos**[1]

[1]Composites and Advanced Materials Centre, School of Aerospace, Transport and Manufacturing, Cranfield University, Bedfordshire, United Kingdom

[2]Biorefining and Advanced Materials Research Centre, Scotland's Rural College (SRUC), Kings Buildings, Edinburgh, United Kingdom

Correspondence
Shouqi Shen, Composites and Advanced Materials Centre, School of Aerospace, Transport and Manufacturing, Cranfield University, Cranfield, Bedfordshire, MK43 0AL, United Kingdom.
Email: shouqi.shen@cranfield.ac.uk

Abstract

This study delineates the dependence of thermophysical behavior of acid-epoxy vitrimers on their formulation. The stress relaxation due to the bond exchange reaction and the glass transition temperature of acid epoxy vitrimers are investigated, with respect to the influence of catalyst content and acid chain length. This is carried out for a range of dicarboxylic acids and catalyst concentrations formulated and characterized using calorimetry and dynamic mechanical analysis. The influence of acid chain length on the bond exchange rate, topological transition, and glass transition temperatures of the vitrimers is found to be significant. The activation energy of the exchange reaction varies over a wide range from 73 to 104 kJ/mol and the topology freezing temperature from 66 to 136°C with the behavior governed by the interplay between crosslinking density, network flexibility and density and distance of functional groups, with an increase of catalyst concentration leading to lower topological transition temperature and the dependence on chain length showing non-monotonic behavior. The glass transition decreases by about 30°C as the carbon chain length increases from 6 to 14 carbons due to enhanced monomer flexibility and is not affected by the concentration of catalyst.

KEYWORDS

differential scanning calorimetry, epoxy, thermal properties, vitrimer

1 | INTRODUCTION

The evolution of polymer science has been markedly influenced by the distinction between thermoplastics and thermosets, historically categorized based on the presence of covalently crosslinked networks. This clear demarcation, however, underwent a paradigm shift with the introduction of covalent adaptable networks (CANs) and the development of vitrimers by Leibler's et al.[1] This class of materials, which blends the robustness of thermosets with the mouldability and recyclability of thermoplastics, has propelled significant advancements in polymer technology. Since then, a range of dynamic covalent linkages, including boronic ester,[2–5] dioxaborolane metathesis,[6–8] and sulphide[9–12] containing reversible exchange, have been extensively explored targeting self-healing materials and groundbreaking biomedical applications.[13–15] Complementing these developments,

This is an open access article under the terms of the Creative Commons Attribution License, which permits use, distribution and reproduction in any medium, provided the original work is properly cited.
© 2024 The Author(s). *Journal of Applied Polymer Science* published by Wiley Periodicals LLC.

transesterification-based epoxy vitrimers, have garnered significant interest due to their excellent properties, versatility, and promising market potential.

Among the wide range of applications of traditional epoxy thermosets, bisphenol A diglycidyl ether (BADGE or DGEBA) dominates the market[16] taking up to 90% of the global conventional production which exceeds 2 million tons worldwide.[17] These traditional epoxy resins have been instrumental in various industries, from the aerospace to the automotive, marine and energy sectors, owing to their favorable mechanical performance, environmental resistance, processability, robust bonding capabilities[18] and insulating properties.[19] The versatility of epoxy resin formulations includes the use of carboxylic acids as curing agents,[20–22] which has led to the development of vitrimers suitable for high-performance applications, including protective coatings and structural components.[18] The increasing demand for high-performance materials that can be tailored for specific applications underscores the need for a deeper understanding of vitrimer chemistry to manipulate their properties at the molecular level.

For functional materials like vitrimers, understanding key characterization temperatures is essential. Similar to conventional thermosetting polymers, vitrimers have a characteristic glass transition temperature (T_g), which defines their safe operational temperature range.[23] However, what sets vitrimers apart is their dynamic nature, driven by bond exchange reactions that allow them to adapt and reconfigure, primarily in response to thermal stimuli. This leads to another critical temperature - the topology freezing temperature (T_v).[24,25] Above T_v, bond exchange occurs rapidly, endowing vitrimers with the fluidity necessary for reprocessing and recycling; below T_v, these reactions slow down, rendering the material behavior akin to traditional thermosets. T_v is crucial as it not only marks the upper limit for vitrimer usage but also significantly influences their reprocessing capabilities. In the study of adjusting the thermally responsive physical properties of vitrimers, particularly those based on transesterification, it is essential to consider the bond exchange reactions, which are typically quite slow and often necessitate the aid of external catalysis. This requirement makes the selection and adjustment of the type and amount of catalyst in the vitrimer system the most common approach to optimize their properties. Among the catalysts employed in transesterification reactions, organometallic complexes such as tin or zinc organic salts and bases such as triazabicyclodecene (TBD) and triphenylphosphine (PPh3) are prevalent. The activation energy for these catalysts, namely TBD, zinc acetylacetonate ($Zn(acac)_2$), zinc(II)acetate ($Zn(OAc)_2$), and PPh3, is 106, 104, 86, and 43 kJ/mol respectively.[26,27]

In this study, zinc acetylacetonate was selected as a catalyst due to its thermal stability and effectiveness in catalyzing transesterification reactions.[1,24,28-31] Zinc-based catalysts, such as zinc acetate, are recognized for their limited environmental impact[32-35] and ability to catalyze reactions even at low concentrations, making them suitable for sustainable materials development. The concentrations of 1 mol%, 2.5 mol%, and 5 mol% were selected to systematically investigate the influence of catalyst concentration on vitrimers properties. These concentrations cover a range from low to relatively high levels, allowing observation of how varying catalyst amounts impact the curing process, stress relaxation behavior, and glass transition temperature. This range provides a comprehensive understanding of the catalyst role, enabling optimization of material properties. Additionally, these concentrations fall within the typical range of 1%–10% used in literature, ensuring comparability with previous studies.[36-40]

Beyond the modification of catalysts and the nature of exchangeable bonds, the intrinsic molecular structure of the polymer chain offers an avenue for tuning vitrimer properties. In the design of vitrimers, changing the structure of the monomers without changing the chemistry of the exchangeable bonds usually aims to change the flexibility of polymer chains which is governed by factors such as chemical structure, side group incorporation, and backbone rigidity to affect the rotation or torsion of skeletal bonds. Flexibility can be manipulated by the integration of rigid structures, such as aromatic rings,[41] cyclic structures[42] or flexible segments such as polyethylene,[43] polypropylene glycol[44] and linear aliphatic chains including polyesters,[45] long methylene bridges[46] and polydimethylsiloxane.[47] Vitrimer systems characterized by increased chain flexibility tend to have lower T_g[48] and faster bond exchange rates in dynamic covalent networks, as the chains can more efficiently align for bond exchange. T_v decreases when the molecular weight of flexible linear segments goes up, yet it rises in response to an increase in the molecular weight of rigid segments.[42] While vitrimers are usually amorphous, adding crystallizable segments can increase rigidity as their dynamic nature allows partial crystallization of substances like dense ethylene, which ordinarily would not crystallize.[49,50] Altering the structure of the monomers in vitrimers directly influences the matrix architectural features, particularly the adapted crosslinking density. In conventional thermosets, increasing crosslinking density leads to greater rigidity and brittleness due to the limited mobility of polymer chains. Conversely, lower crosslinking density enhances elasticity and ductility, as fewer junctures allow for greater chain mobility and flexibility.[8] In vitrimers, the dynamic nature of the material creates a

10974628, 0, Downloaded from https://onlinelibrary.wiley.com/doi/10.1002/app.56028 by Test, Wiley Online Library on [25/08/2024]. See the Terms and Conditions (https://onlinelibrary.wiley.com/terms-and-conditions) on Wiley Online Library for rules of use; OA articles are governed by the applicable Creative Commons License

complex interplay with crosslinking density. Steric hindrance, resulting from densely packed chains, can potentially obstruct the bond exchange, a quintessential feature of vitrimers. However, empirical studies have yielded mixed results with both faster relaxation in less crosslinked materials[51,52] and accelerated bond exchange with increased crosslink density[53,54] reported. Such differences in behavior might arise from variations in the concentration and proximity of reactive exchangeable groups concurrent with changes in crosslink density. Hayashi et al.[55] reported enhanced relaxation in transesterification-based vitrimers with higher crosslinking, without altering the concentration of reactive groups. This behavior is attributed to the dominance of unstable, entropically perturbed segments in densely crosslinked networks. The multifaceted relationship between crosslinking density and vitrimer properties necessitates a comprehensive approach in vitrimer design. It is imperative to strike a balance between dynamic covalent processability and the overarching material properties to harness the full potential of vitrimers.

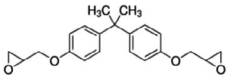
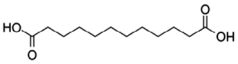
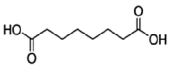
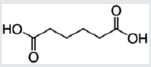
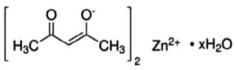
This study presents a detailed investigation of the properties of various epoxy/acid-based vitrimer formulations, focusing on their relaxation behavior, topological freezing temperature and glass transition temperature is carried out using a combination of Differential Scanning Calorimetry (DSC), Dynamic Mechanical Analysis (DMA), and Arrhenius model-based evaluations. To ensure consistent conversion of reactants across different catalyst concentrations, the progress of the synthesis was closely monitored using Fourier Transform Infrared (FTIR) spectroscopy, confirming complete curing in all samples. Our unique contribution lies in elucidating the influence of both catalyst concentration and structural variations of acid chains on vitrimer properties, thus offering new insights into the complex interplay between these factors and their impact on vitrimer behavior.

2 | MATERIALS AND METHODS

Diepoxy (DGEBA), five linear dicarboxylic acids with different chain length, and $Zn(acac)_2$ as a transesterification catalyst were used in the synthesis of the vitrimer systems. The properties of the chemicals are summarized in Table 1. All chemicals were sourced from Merck Life Science UK Limited.

Acid crystals were ground to a fine powder to ensure uniform acid dispersion in the epoxy. Stoichiometric proportions of acids and epoxy were weighed, and three concentrations of $Zn(acac)_2$ catalyst (1 mol%, 2.5 mol%, and 5 mol%) were incorporated, yielding 15 distinct vitrimer formulations. The epoxy, acid, and catalyst were combined and stirred to obtain homogeneous mixtures. The mixtures were degassed at 90°C for an hour to remove air entrapped during mixing, then cast in rubber-sealed glass molds. The samples were subsequently cured at 160°C for 2 h, maintaining a 1:1 functional group ratio of epoxy to acid. Formulation names were based on the acid carbon chain length, for example, C6Z2.5 denotes adipic acid with 2.5 mol% $Zn(acac)_2$. Table 2 summarizes the details of the formulations.

TABLE 1 Details of chemicals used in vitrimer formulations.

Chemical structure	Compound	Molecular mass (g/mol)
	Bisphenol A diglycidyl ether (D.E.R.™ 332)	340.4
	Tetradecanedioic acid	258.35
	Dodecanedioic acid	230.30
	Sebacic acid	202.25
	Suberic acid	174.19
	Adipic acid	146.14
	Zinc acetylacetonate hydrate	263.61

The stress relaxation behavior of the vitrimer materials was assessed using Dynamic Mechanical Analysis (DMA) on a TA Instruments DMA Q800. Rectangular specimens measuring 2 mm × 40 mm × 10 mm were subjected to single cantilever mode tests at a fixed strain of 2.5% and allowed to relax until the stress reached a value below 37% of the initial value. The tests were performed across various temperatures to investigate the temperature dependence of bond exchange. DMA relaxation tests were repeated three times. The relaxation time (τ^*) was determined by fitting an exponential decay:

$$\frac{\sigma}{\sigma_0} = e^{-\frac{t}{\tau}} \quad (1)$$

where σ is the stress at time t and σ_0 is the stress at the beginning of the relaxation. The relaxation time was estimated by minimizing the error between the experimental data and Equation (1) using the Generalized Reduced Gradient Nonlinear Optimisation method implemented in the Solver of Microsoft Excel.[56]

10974628, 0, Downloaded from https://onlinelibrary.wiley.com/doi/10.1002/app.56028 by Test, Wiley Online Library on [25/08/2024]. See the Terms and Conditions (https://onlinelibrary.wiley.com/terms-and-conditions) on Wiley Online Library for rules of use; OA articles are governed by the applicable Creative Commons License

TABLE 2 Composition of the vitrimer materials.

Material code	$Zn(acac)_2$ content (%mol)	Acid	Epoxy
C6Z1	1.0	Adipic acid ($C_6H_{10}O_4$)	DGEBA
C6Z2.5	2.5		
C6Z5	5.0		
C8Z1	1.0	Suberic acid ($C_8H_{14}O_4$)	DGEBA
C8Z2.5	2.5		
C8Z5	5.0		
C10Z1	1.0	Sebacic acid ($C_{10}H_{18}O_4$)	DGEBA
C10Z2.5	2.5		
C10Z5	5.0		
C12Z1	1.0	Dodecanedioic acid ($C_{12}H_{22}O_4$)	DGEBA
C12Z2.5	2.5		
C12Z5	5.0		
C14Z1	1.0	Tetradecanedioic acid ($C_{14}H_{26}O_4$)	DGEBA
C14Z2.5	2.5		
C14Z5	5.0		

The stress relaxation behavior of vitrimers Is influenced by the bond exchange rate in the dynamic cross-links. This temperature-relaxation relationship follows an Arrhenius law:

$$\tau = \frac{1}{K_0} e^{\frac{E_{ar}}{RT}} \quad (2)$$

where the pre-exponential factor K_0 represents the frequency of collisions and E_{ar} is the activation energy. The activation energy for transesterification bond exchange was estimated as the gradient of logarithmic relaxation time versus inverse absolute temperature (T). Previous work has shown that the mechanism of lowering the energy barrier remains consistent for a specific type of bond exchange associated with a particular catalyst, and is unaffected by variations in catalyst concentration.[25,57,58] In the analysis carried in this work the 9 data points corresponding to same acid (3 formulations corresponding to different catalyst concentrations tested at 3 different temperatures) were utilized to obtain a single activation energy for the acid type involved. The topology freezing transition temperature T_v was determined as the temperature at which the relaxation time is 10^6 s for each formulation.

Differential Scanning Calorimetry (DSC) was performed with a TA Instruments Discovery DSC 250 to identify the glass transition temperature. Materials were tested under a nitrogen flow at a heating rate of 2°C/min from −10 to 60°C. Experiments were repeated three times to allow assessment of statistical significance of differences.

Fourier Transform Infrared (FTIR) spectra were obtained using a Thermo Scientific Nicolet™ iS™10 FT-IR spectrometer. The IR data of DGEBA, catalyst, all acids, and mixtures before and after curing were collected in the range of 600–4000 cm^{-1}. For each spectrum, 50 consecutive scans with a resolution of 4 cm^{-1} were averaged; all spectra were recorded at room temperature.

The dataset underlying this study is available at the Cranfield online research data repository.[59]

3 | RESULTS AND DISCUSSION

3.1 | Synthesis progress and FTIR monitoring

To ensure consistent conversion of reactants across different catalyst concentrations, the progress of the synthesis was closely monitored using Fourier Transform Infrared (FTIR) spectroscopy. The catalyst plays a dual role in the systems: it initiates the ring opening of the epoxy during the polymerization of uncured reactants and aids in transesterification. The FTIR results presented in Figure 1 show the disappearance of epoxy groups, indicated by the reduction of the characteristic epoxy peak at 910 cm^{-1}, and the concurrent increase of hydroxyl and ester groups, evidenced by the rise of the OH peak at 3450 cm^{-1} and the shift of the C=O stretching bands from 1690 to 1735 cm^{-1} due to the loss of the stabilizing hydroxyl group from carboxylic acids to esters. This phenomenon is consistently observed in formulations with

10974628, 0, Downloaded from https://onlinelibrary.wiley.com/doi/10.1002/app.56028 by Test, Wiley Online Library on [25/08/2024]. See the Terms and Conditions (https://onlinelibrary.wiley.com/terms-and-conditions) on Wiley Online Library for rules of use; OA articles are governed by the applicable Creative Commons License

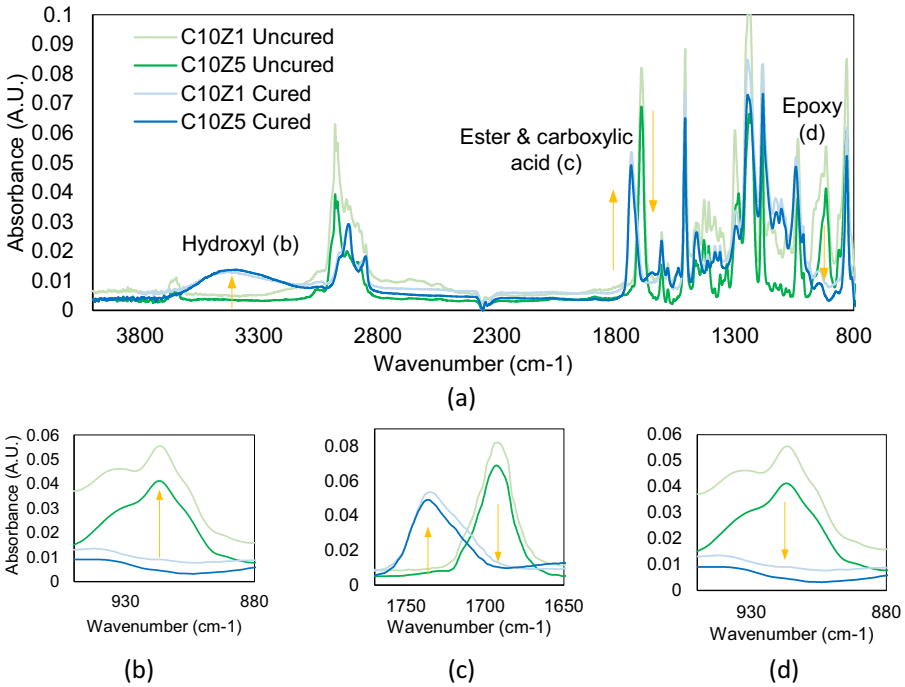


FIGURE 1 FTIR spectra of cured and uncured vitrimers for formulation C10: (a) overall spectrum; (b) hydroxyl group in 3700–3100 cm^{-1}; (c) ester group in 1800–1650 cm^{-1}; and (d) epoxy group in 990–880 cm^{-1}. [Color figure can be viewed at wileyonlinelibrary.com]

both low and high catalyst content. During the curing process, the additional catalyst accelerates the cure process[61] and influences the time required for the system to reach full curing. However, complete cure is achieved by the end of the reaction for all formulations, meaning that the final degree of crosslinking is the same for formulations with the same acid and epoxy composition regardless of their catalyst level. Furthermore, homopolymerisation of the epoxy is precluded during the manufacturing process for all formulations, irrespective of catalyst concentration, due to insufficient reaction temperature to trigger this process.[60] Should homopolymerisation occur, it would lead to an increase in T_g.

3.2 | Stress relaxation and topology freezing temperature

Figure 2a illustrates the stress relaxation of C12Z2.5 (epoxy-dodecanedioic acid with 2.5% catalyst) at three different temperatures. The relaxation time reduces from about 14,000 to 750 s when the temperature increases from 140°C to 180°C, a difference exceeding one order of magnitude, which is typical across all formulations. Figure 2b illustrates the relaxation behavior of vitrimers C6 (adipic acid), C8 (suberic acid), and C10 (sebacic acid) with 1% and 5% catalyst at 230°C. The relaxation times vary significantly, ranging from a brief 150 s (C10Z5) to an extended 3650 s (C8Z1), demonstrating a pronounced dependence on the catalyst and acid structure. Notably, when the catalyst concentration

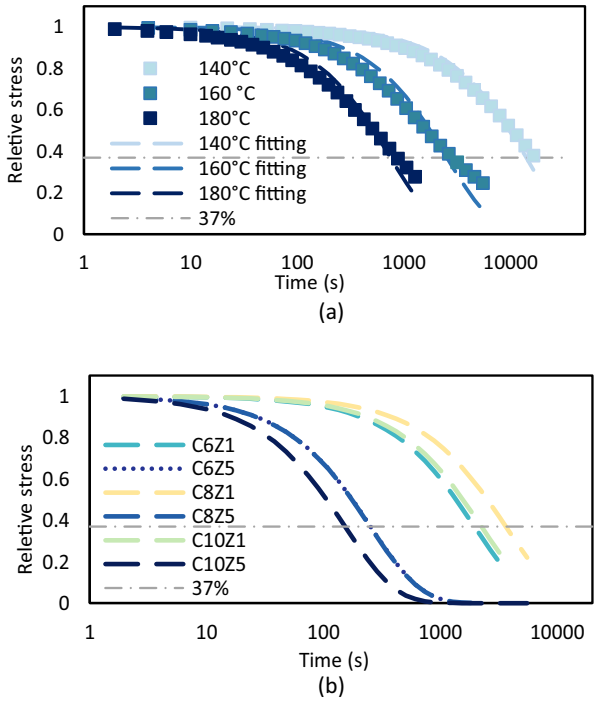


FIGURE 2 Normalized stress relaxation curves of (a) dodecanedioic acid vitrimer with 2.5% catalyst at 140, 160 and 180°C; (b) adipic, suberic and sebacic acid formulations at 230°C. [Color figure can be viewed at wileyonlinelibrary.com]

increases from 1% to 5%, the relaxation times decrease by more than one order of magnitude. Meanwhile, there is a comparatively smaller difference—less than 50%—across three different formulations that use the same

10974628, 0, Downloaded from https://onlinelibrary.wiley.com/doi/10.1002/app.56028 by Test, Wiley Online Library on [25/08/2024]. See the Terms and Conditions (https://onlinelibrary.wiley.com/terms-and-conditions) on Wiley Online Library for rules of use; OA articles are governed by the applicable Creative Commons License

catalyst concentration but vary in their acid compositions. The results of the fitting for the estimation of the activation energy and pre-exponential factor of Equation (2) are reported in Table 3.

Figure 3 illustrates the Arrhenius fitting for all formulations. The fitting follows experimental results closely with a coefficient of determination (R^2) of 0.96 throughout all formulations. For the transesterification reaction catalyzed by $Zn(acac)_2$, the reported E_{ar} varies from 24 to 163 kJ/mol.[61,62] The range observed in this study is 73–108 kJ/mol with the value of activation energy showing a strong dependence on acid chain length. The activation energy for viscous flow indicates how temperature changes affect the viscosity of associative CANs. Higher E_{ar} values lead to a rapid decrease in viscosity with increasing temperature, while lower E_{ar} values result in less pronounced changes. High E_{ar} systems offer improved dimensional stability at service temperatures and enable fast processing at reprocessing temperatures.

As depicted in Figure 4, as the chain length extends, the activation energy initially rises from the lowest value for C6 (adipic acid) to a maximum for C8 (suberic acid) and then showing a decreasing trend with increasing chain length. Figure 4b presents the obtained T_v for all vitrimers showing a decreasing trend with increasing catalyst levels and an increase-plateau-decrease pattern as a function of acid chain length. The overall range in topology freezing temperatures observed is 66–136°C. T_v

TABLE 3 Relaxation fitting parameters.

Material		C6	C8	C10	C12	C14
(E_{ar}/R) (K)		8833	12,945	11,808	12,009	10,459
Ln $(1/K_0)$ (s)	1.0%	−9.6	−17.8	−15.9	−16.6	−14.3
	2.5%	−10.9	−18.6	−16.7	−19.8	−16.1
	5.0%	−12.2	−20.5	−18.6	−20.8	−16.5

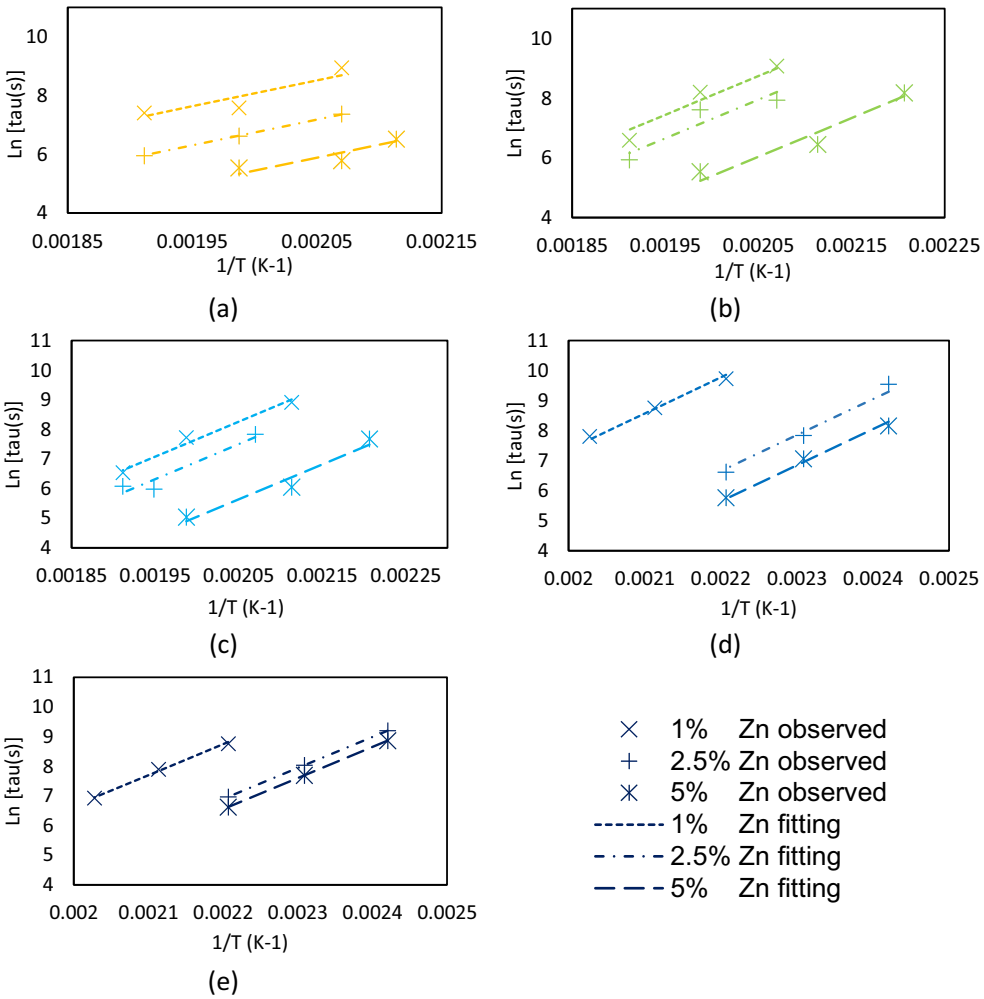


FIGURE 3 Stress relaxation Arrhenius fitting: (a) C6; (b)C8; (c) C10; (d) C12; (e) C14. [Color figure can be viewed at wileyonlinelibrary.com]

10974628, 0, Downloaded from https://onlinelibrary.wiley.com/doi/10.1002/app.56028 by Test, Wiley Online Library on [25/08/2024]. See the Terms and Conditions (https://onlinelibrary.wiley.com/terms-and-conditions) on Wiley Online Library for rules of use; OA articles are governed by the applicable Creative Commons License

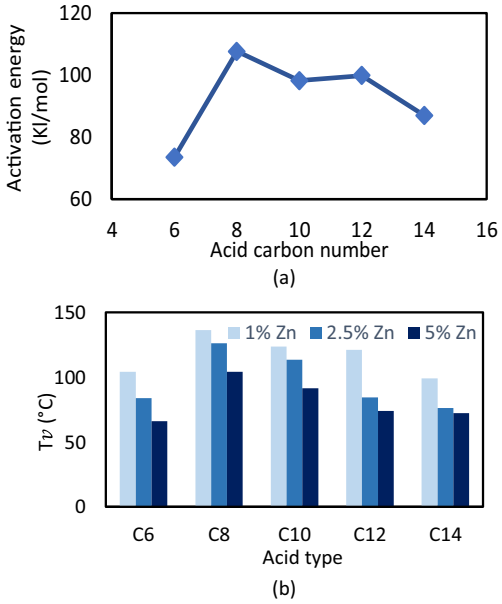


FIGURE 4 Activation energy (a) and topology freezing temperature; (b) for all vitrimer formulations as a function of chain length. [Color figure can be viewed at wileyonlinelibrary.com]

increases by about 30–40°C from adipic (C6) to suberic (C8) acid for the same level of catalyst concentration and then it reduces by about 6°C per methylene unit at the same level of catalyst. For vitrimer formulations using the same acid, a decrease of about 32–47°C is observed when the catalyst concentration increases from 1% to 5%.

Figure 5 illustrates the transesterification bond exchange between the hydrolyzed epoxy and ester groups. The macroscopic flow and stress relaxation behavior is the result of the bond exchange reaction. The speed of the reaction is determined by two factors: (i) the amount of the reacting groups; and (ii) the accessibility to them. Taking into consideration the molecular structure and the reaction pattern, there are five factors that influence the bond exchange rate: (i) amount of hydroxyl and ester groups; (ii) chain flexibility; (iii) catalyst concentration; (iv) crosslinking density; and (v) the statistical distance between reaction groups.[63] The presence of the catalyst provides a pathway for the reaction to happen with a lower energy barrier by activating both the ester and alcohol groups simultaneously.[64] The mechanism of lowering the energy barrier remains consistent for a specific type of bond exchange associated with a particular catalyst. This is characterized by a constant activation energy, which remains unchanged despite variations in catalyst concentration.[25,57,58] Although an increase in catalyst content provides more sites for bond exchange, thereby increasing the overall rate of transesterification, the impact of the other four factors—chain flexibility, crosslinking density, and the statistical distance between reaction groups, in addition to the amount of hydroxyl and ester groups—is also crucial. These factors also affect the probability of the reaction occurring, which explains the irregular activation energy trend shown in Figure 4a as the acid chain length increases. The effects of these factors on the bond exchange rate are summarized in Table 4.

Figure 6 illustrates the difference in the crosslinks of vitrimers constructed with dicarboxylic acids with different chain length. At the molecular level, in terms of spatial arrangement and configuration, the crosslinked network created by diepoxy and linear dicarboxylic acid, featuring longer linear chain segments of varied methylene repetition, results in fewer crosslinks within the same space. This structure facilitates the movement of hydroxyl ends and ester groups through the network, making it easier for them to interact and complete the transesterification process. Additionally, longer chains bring more flexibility to the backbone which grants more adaptability to the backbone to change its configuration. Conversely, lengthening the chain introduces two factors that inhibit bond exchange: a reduction in the relative density of functional groups and an increased distance that exchangeable ends must travel to take part in the reaction.

Among all the formulations, C6 (adipic acid) which has the shortest linear methylene repetition in the chain, exhibits the fastest stress relaxation and bond exchange, along with the lowest corresponding T_v when 5 mol% catalyst is present. This vitrimer has the highest functional group density and the shortest travel distance, promoting localized and vigorous bond exchange. Consequently, the potential hindrance of diffusion, resulting from high crosslink density and stiff chains, are comparatively less significant. The fact that vitrimers synthesized using suberic acid and sebacic acid (formulations C8 and C10) have the highest T_v and the decreasing trend after that, indicates that when gradually increasing the length of the acid chain, at first, the end-to-end distance plays a more significant role in the transesterification reaction. This is due to the greater relative difference created by the addition of chain length, considering the short repeating units. This effect is attenuated as the number of methylene groups increases further. At the same time, the reduction in crosslinking density and the presence of longer chains allow more flexibility within the network. This effect overrides the influence of the increase in reaction end distance and of the decrease in functional group density. A similar influence of the longer alkyl chains on T_v is reported by Yang et al.[23] where a 12°C drop in T_v was observed between epoxy vitrimers cured by dodecanedioic acid and octadecanedioic acid with the same catalyst content. As the chain length increases continuously,

10974628, 0, Downloaded from https://onlinelibrary.wiley.com/doi/10.1002/app.56028 by Test, Wiley Online Library on [25/08/2024]. See the Terms and Conditions (https://onlinelibrary.wiley.com/terms-and-conditions) on Wiley Online Library for rules of use; OA articles are governed by the applicable Creative Commons License

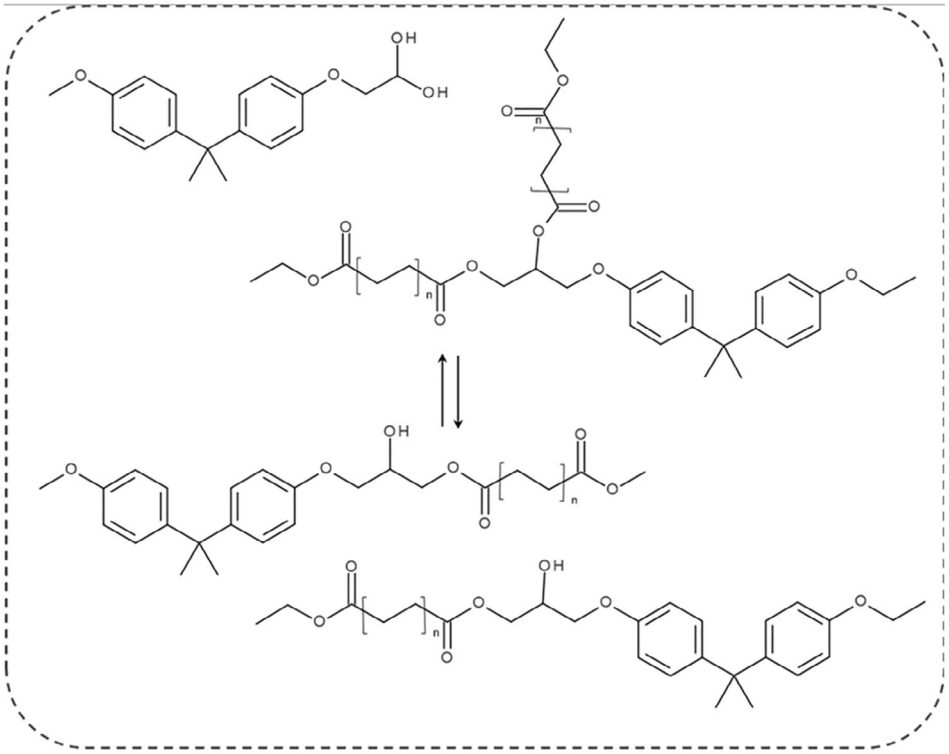


FIGURE 5 Exchange process via transesterification in hydroxy-ester networks.

TABLE 4 Influence of increasing methylene groups in acid chains on bond exchange rate.

Factor	Effect of increasing acid chain	Effect on bond exchange
Crosslink density	↓	↑
Chain flexibility	↑	↑
Functional groups	↓	↓
Groups distance	↑	↓

and the molecular weight of the backbone between exchangeable crosslinks reaches a certain level, there is a threshold beyond which the change in chain length no longer affects the entanglement or flow rate of the network but instead dilutes the density of reaction ends.[65] This leads to a decrease in the bond exchange rate, resulting in slower stress relaxation and a higher T_v.

3.3 | Glass transition behavior

Figure 7a illustrates the DSC thermograms showing a considerable variation in T_g values between the formulations synthesized using different acids, except for C12 and C14. The dependence of the glass transition temperature on acid chain length is depicted in Figure 7b. There is a trend of decreasing T_g with increasing number of methylene repetitions, with a drop of about 30°C from adipic acid (6 carbon) to dodecanedioic acid (12 carbons). The trend diminishes from 12 to 14 carbon units. The materials made with the same acid show only a slight variation in T_g with varying catalyst concentration. The spread of values for the same acid is around 3°C which, when compared with the standard deviation ranging from about 1 to 2.5°C, indicates no statistical significance. Therefore, it can be concluded that within the range of catalyst concentrations used in this study, the glass transition temperature of the materials is predominantly influenced by the monomer structure rather than the catalyst concentration.

The decreasing trend of glass transition temperature as a function of acid length can be attributed to the differences in network structure. The size of the molecules increases with increasing acid length, resulting in a reduction of crosslinking density. Lower crosslinking density results in a lower T_g. The overall qualitative characteristics of the structure of the acids are the same, meaning that no variation in branches, rigid building blocks, or cyclic structures cause a difference in the T_g of the different formulations. The enhanced flexibility causes a lower energy requirement to overcome intermolecular forces and facilitates the transition of the material from a rigid, glassy state to a more flexible, rubbery state. Such a phenomenon has been reported for an epoxy resin and diamines with different length of oxypropylene units.[66] The decreasing trend is not followed in the case of the C12 and C14, which have similar glass transition temperatures within the limits of statistical variation.

10974628, 0, Downloaded from https://onlinelibrary.wiley.com/doi/10.1002/app.56028 by Test, Wiley Online Library on [25/08/2024]. See the Terms and Conditions (https://onlinelibrary.wiley.com/terms-and-conditions) on Wiley Online Library for rules of use; OA articles are governed by the applicable Creative Commons License

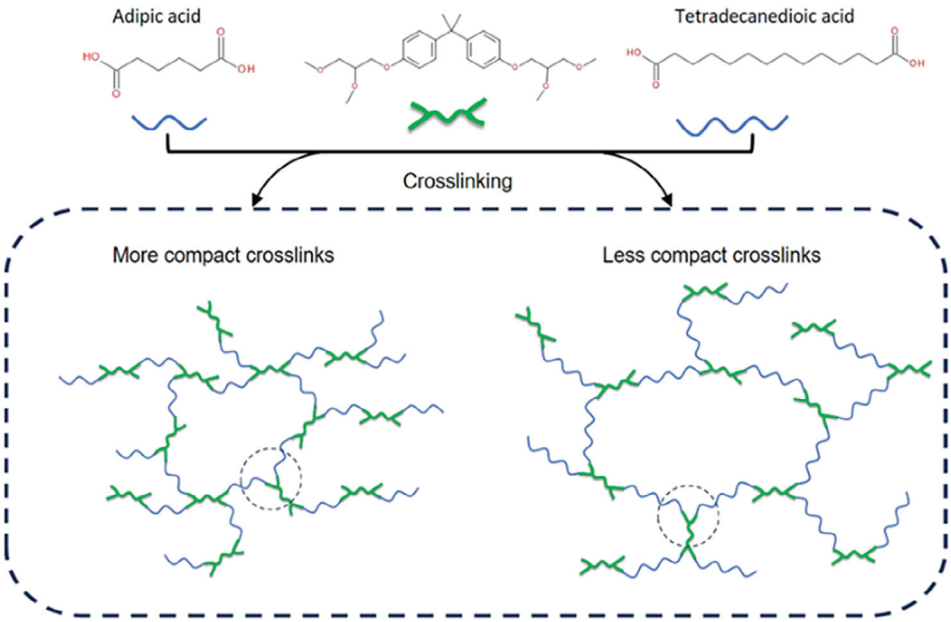


FIGURE 6 Difference in the crosslinked structure of vitrimer made of linear dicarboxylic acid with varied number of methylene groups. [Color figure can be viewed at wileyonlinelibrary.com]

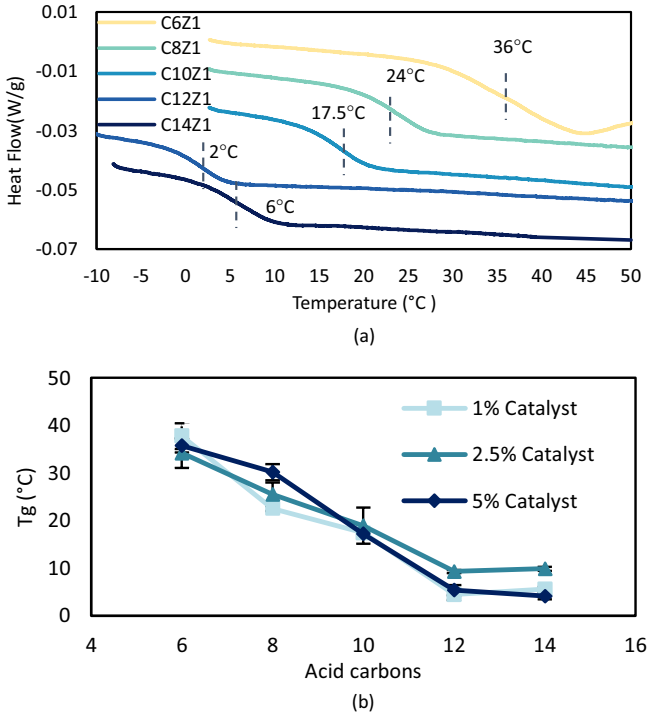


FIGURE 7 (a) DSC results and (b) glass transition temperature of vitrimers with different carboxylic acids. [Color figure can be viewed at wileyonlinelibrary.com]

This can be attributed to a diminishing effect of the influence of reduction of crosslinking density below a lever as other phenomena related to intermolecular forces and chain flexibility dominate. The results indicate that within the experimental conditions and catalyst concentrations used, the glass transition temperature of the formulations is primarily dependent on the monomer structure and shows minimal variation with changes in catalyst concentration.

In addition to the observed trends in T_g, the estimated relaxation time for all the formulations at their respective glass transition temperature ranges from 1.30×10^7 s to 3.65×10^{11} s, showing a decrease with increasing catalyst content. However, DSC tests conducted have a timescale in the order of 10^3 s. Even the shortest relaxation time is four orders of magnitude longer. Therefore, bond exchange around a temperature much lower than the topology transition temperature is likely to be insignificant in altering the glass transition behavior. However, an extended measurement of T_g over an extremely slow temperature ramp may reveal some dependence between catalyst concentration and T_g.

4 | CONCLUSION

The relaxation behavior of the formulations investigated shows an increase-plateau-decrease pattern of the topological freezing temperature in relation to chain length due to the combined effects of the change in the amount and accessibility of reacting groups, chain flexibility, crosslinking density, and distance between reaction groups. An increase in repetitions of the acid molecule correlates with a reduction in T_g, stabilizing beyond a chain length of 12 methylene units as a result of reduced crosslinking density and enhanced chain flexibility. T_g does not have a dependence on catalyst content, since completion of cure occurs even for formulations that react slowly, whilst bond exchange is extremely slow in the range of the glass transition temperatures. The glass

10974628, 0, Downloaded from https://onlinelibrary.wiley.com/doi/10.1002/app.56028 by Test, Wiley Online Library on [25/08/2024]. See the Terms and Conditions (https://onlinelibrary.wiley.com/terms-and-conditions) on Wiley Online Library for rules of use; OA articles are governed by the applicable Creative Commons License

transition of vitrimers mostly depends on the flexibility of the chain and the crosslinking density of the polymer. On the other hand, the topology transition behavior is determined by a greater set of parameters. The results reported here demonstrate the wide range of possibilities for the tailoring of vitrimers, enabling control over their properties for specific applications.

AUTHOR CONTRIBUTIONS

Shouqi Shen: Conceptualization (lead); data curation (lead); formal analysis (lead); investigation (lead); methodology (lead); project administration (lead); software (lead); validation (lead); visualization (lead); writing – original draft (lead); writing – review and editing (equal). **Vijay K. Thakur:** Conceptualization (supporting); supervision (supporting). **Alex Skordos:** Conceptualization (supporting); data curation (supporting); formal analysis (supporting); methodology (supporting); software (supporting); supervision (lead); validation (supporting); writing – review and editing (equal).

CONFLICT OF INTEREST STATEMENT

The authors declare no conflicts of interest.

DATA AVAILABILITY STATEMENT

Electronic Supplementary Information (ESI) includes Differential Scanning Calorimetry (DSC) datafor all cured formulations, Fourier Transform Infrared Spectroscopy (FTIR) of samples pre- and post-crosslinking, and Dynamic Mechanical Analysis (DMA) stress relaxation data at three temperatures per formulation. Available at the Cranfield research data repository: [https://doi.org/10.60927/vk9n-m902].

ORCID

Shouqi Shen https://orcid.org/0000-0003-2314-7470
Alexandros A. Skordos https://orcid.org/0000-0003-1273-029X

REFERENCES

[1] D. Montarnal, M. Capelot, F. Tournilhac, L. Leibler, *Science* **2011**, *334*, 965.
[2] A. P. Bapat, D. Roy, J. G. Ray, D. A. Savin, B. S. Sumerlin, *J. Am. Chem. Soc.* **2011**, *133*, 19832.
[3] B. M. Dufort, M. W. Tibbitt, *Mater. Today Chem.* **2019**, *12*, 16.
[4] O. R. Cromwell, J. Chung, Z. Guan, *J. Am. Chem. Soc.* **2015**, *137*, 6492.
[5] S. Wang, X. Xing, X. Zhang, X. Wang, X. Jing, *J. Mater. Chem. A* **2018**, *6*, 10868.
[6] F. Caffy, R. Nicolaÿ, *Polym. Chem.* **2019**, *10*, 3107.
[7] M. Röttger, T. Domenech, R. Van Der Weegen, A. Breuillac, R. Nicolaÿ, L. Leibler, *Science* **2017**, *356*, 62.
[8] A. Breuillac, A. Kassalias, R. Nicolaÿ, *Macromolecules* **2019**, *52*, 7102.
[9] Z. Ma, Y. Wang, J. Zhu, J. Yu, Z. Hu, *J. Polym. Sci. Part A Polym. Chem.* **2017**, *55*, 1790.
[10] Y. Amamoto, H. Otsuka, A. Takahara, K. Matyjaszewski, *Adv. Mater.* **2012**, *24*, 3975.
[11] A. Rekondo, R. Martin, A. Ruiz De Luzuriaga, G. Cabañero, H. J. Grande, I. Odriozola, *Mater. Horizons* **2014**, *1*, 237.
[12] Z. Guo, B. Liu, L. Zhou, L. Wang, K. Majeed, B. Zhang, F. Zhou, Q. Zhang, *Polymer* **2020**, *197*, 122483.
[13] D. G. Hall, *Chem. Soc. Rev.* **2019**, *48*, 3475.
[14] W. L. A. Brooks, B. S. Sumerlin, *Chem. Rev.* **2016**, *116*, 1375.
[15] S. P. Black, J. K. M. Sanders, A. R. Stefankiewicz, *Chem. Soc. Rev.* **2014**, *43*, 1861.
[16] C. J. Kloxin, T. F. Scott, B. J. Adzima, C. N. Bowman, *Macromolecules* **2010**, *43*, 2643.
[17] H. Jiang, L. Sun, Y. Zhang, F. Meng, W. Zhang, C. Zhao, *Eur. Polym. J.* **2018**, *108*, 507.
[18] R. W. Hewitt, Epoxy Resins, vol. 28, no. 8. Routledge. **1970**.
[19] H. S. Kaufman, *J. Appl. Polym. Sci.* **1970**, *14*, 253.
[20] N. V. Tsarevsky, S. A. Bencherif, K. Matyjaszewski, *Macromolecules* **2007**, *40*, 4439.
[21] K. D. Libor Matějka, S. Pokorný, *Macromol. Chem. Phys.* **1985**, *186*, 229.
[22] L. Matějka, K. Dušek, *Polym. Bull.* **1986**, *15*, 215.
[23] Y. Yang, S. Zhang, X. Zhang, L. Gao, Y. Wei, Y. Ji, *Nat. Commun.* **2019**, *10*, 1.
[24] M. Capelot, D. Montarnal, F. Tournilhac, L. Leibler, *J. Am. Chem. Soc.* **2012**, *134*, 7664.
[25] M. Capelot, M. M. Unterlass, F. Tournilhac, L. Leibler, *ACS Macro Lett.* **2012**, *1*, 789.
[26] A. Kumar, L. A. Connal, *Macromol. Rapid Commun.* **2023**, *44*, 2200892.
[27] W. Denissen, J. M. Winne, F. E. Du Prez, *Chem. Sci.* **2016**, *7*, 30.
[28] H. Jiarui, T. Liu, S. Zhang, C. Hao, J. Xin, B. Guo, J. Zhang, *Ind. Eng. Chem. Res.* **2019**, *58*, 6466.
[29] B. Zhang, K. Kowsari, A. Serjouei, M. L. Dunn, Q. Ge, *Nat. Commun.* **2018**, *9*, 1831.
[30] A. Legrand, C. Soulié-Ziakovic, *Macromolecules* **2016**, *49*, 5893.
[31] G. Zhang, X. Zhou, K. Liang, B. Guo, X. Li, Z. Wang, L. Zhang, *ACS Sustainable Chem. Eng.* **2019**, *13*, 11712.
[32] M. Rani, J. Y. Keshu, U. Shanker, *Zinc-Based Nanostructures for Environmental and Agricultural Applications*, Elsevier, Amsterdam, **2021**, p. 93.
[33] R. Tayebee, S. Javad Ahmadi, E. R. Seresht, F. Javadi, M. A. Yasemi, M. Hosseinpour, B. Maleki, *Ind. Eng. Chem. Res.* **2012**, *51*, 14577.
[34] N. A. Hussien, J. S. Al Malki, F. A. R. Al Harthy, A. W. Mazi, J. A. A. Al Shadadi, *Sustainability* **2023**, *15*, 9864.
[35] F. A. M. Alahdal, M. T. A. Qashqoosh, Y. K. Manea, M. A. S. Salem, A. M. T. Khan, S. Naqvi, *OpenNano* **2022**, *8*, 100067.
[36] J. Joe, J. Shin, Y. S. Choi, J. H. Hwang, S. H. Kim, J. Han, D. G. Kim, *Adv. Sci.* **2021**, *8*, 2103682.
[37] R. Korotkov, V. Shutov, A. Orlov, N. Bornosuz, D. Kulemza, D. Onuchin, A. Shcherbina, I. Gorbunova, I. Sirotin, *Polymer* **2024**, *16*, 392.
[38] M. Giebler, C. Sperling, S. Kaiser, I. Duretek, S. Schlögl, *Polymer* **2020**, *12*, 1148.
[39] S. Zhang, T. Liu, C. Hao, L. Wang, J. Han, H. Liu, J. Zhang, *Green Chem.* **2018**, *20*, 2995.

10974628, 0, Downloaded from https://onlinelibrary.wiley.com/doi/10.1002/app.56028 by Test, Wiley Online Library on [25/08/2024]. See the Terms and Conditions (https://onlinelibrary.wiley.com/terms-and-conditions) on Wiley Online Library for rules of use; OA articles are governed by the applicable Creative Commons License

[40] C. Brondi, A. Marotta, G. Filippone, G. Mensitieri, M. Salzano de Luna, V. Ambrogi, *Macromol. Chem. Phys.* **2023**, *224*, 2300273.
[41] H. Zheng, Q. Liu, X. Lei, Y. Chen, B. Zhang, Q. Zhang, *J. Mater. Sci.* **2019**, *54*, 2690.
[42] C. He, P. R. Christensen, T. J. Seguin, E. A. Dailing, B. M. Wood, R. K. Walde, K. A. Persson, T. P. Russell, B. A. Helms, *Angew. Chem. – Int. Ed.* **2020**, *59*, 735.
[43] W.-G. Hu, K. Schmidt-Rohr, *Acta Polym.* **1999**, *50*, 271.
[44] I. Azcune, A. Huegun, A. Ruiz de Luzuriaga, E. Saiz, A. Rekondo, *Eur. Polym. J.* **2021**, *148*, 110362.
[45] M. Bouyahyi, M. P. F. Pepels, A. Heise, R. Duchateau, *Macromolecules* **2012**, *45*, 3356.
[46] F. Meng, M. O. Saed, E. M. Terentjev, *Macromolecules* **2019**, *52*, 7423.
[47] R. G. Ricarte, S. Shanbhag, *Macromolecules* **2021**, *54*, 3304.
[48] M. Chen, L. Zhou, Y. Wu, X. Zhao, Y. Zhang, *ACS Macro Lett.* **2019**, *8*, 255.
[49] K. Saalwächter, B. Soman, C. M. Evans, *Front. Soft Matter* **2023**, *3*, 1208777.
[50] B. Soman, Y. K. Go, C. Shen, C. Leal, C. M. Evans, *Soft Matter* **2022**, *18*, 293.
[51] J. P. Brutman, D. J. Fortman, G. X. De Hoe, W. R. Dichtel, M. A. Hillmyer, *J. Phys. Chem. B* **2019**, *123*, 1432.
[52] S. Zhao, M. M. Abu-Omar, *Macromolecules* **2019**, *52*, 3646.
[53] M. M. Obadia, A. Jourdain, P. Cassagnau, D. Montarnal, E. Drockenmuller, *Adv. Funct. Mater.* **2017**, *27*, 1.
[54] M. Hayashi, R. Yano, A. Takasu, *Polym. Chem.* **2019**, *10*, 2047.
[55] M. Hayashi, R. Yano, *Macromolecules* **2020**, *53*, 182.
[56] D. Fylstra, L. Lasdon, J. Watson, A. Waren, *Interfaces* **1998**, *28*, 29.
[57] R. Long, H. J. Qi, M. L. Dunn, *Soft Matter* **2013**, *9*, 4083.
[58] G. M. Scheutz, J. J. Lessard, M. B. Sims, B. S. Sumerlin, *J. Am. Chem. Soc.* **2019**, *141*, 16181.
[59] S. Shen, V. K. Thakur, A. A. Skordos, Dataset: Influence of Acid Structure and Catalyst Concentration on the Relaxation and Glass Transition and Relaxation of Dicarboxylic Acid-Epoxy Vitrimers, Cranfield Online Research Data Repository, https://doi.org/10.60927/vk9n-m902.
[60] J. M. Morancho, X. Ramis, X. Fernández-Francos, O. Konuray, J. M. Salla, *J. Therm. Anal. Calorim.* **2020**, *142*, 607.
[61] S. Zhao, M. M. Abu-Omar, *Macromolecules* **2019**, *52*, 3646.
[62] A. Jourdain, R. Asbai, O. Anaya, M. M. Chehimi, E. Drockenmuller, D. Montarnal, *ACS Appl. Mater. Interfaces* **2020**, *53*, 1884.
[63] J. Wu, L. Gao, Z. Guo, H. Zhang, B. Zhang, H. Jun, M. H. Li, *Green Chem.* **2021**, *23*, 5647.
[64] J. Kadota, D. Pavlović, J. P. Desvergne, B. Bibal, F. Peruch, A. Deffieux, *Macromolecules* **2010**, *43*, 8874.
[65] J. J. Lessard, K. A. Stewart, B. S. Sumerlin, *Macromolecules* **2022**, *55*, 10052.
[66] S. Montserrat, P. Cortés, Y. Calventus, J. M. Hutchinson, *J. Polym. Sci., Part B: Polym. Phys.* **2000**, *38*, 456.

How to cite this article: S. Shen, V. K. Thakur, A. A. Skordos, *J. Appl. Polym. Sci.* **2024**, e56028. https://doi.org/10.1002/app.56028

10974628, 0, Downloaded from https://onlinelibrary.wiley.com/doi/10.1002/app.56028 by Test, Wiley Online Library on [25/08/2024]. See the Terms and Conditions (https://onlinelibrary.wiley.com/terms-and-conditions) on Wiley Online Library for rules of use; OA articles are governed by the applicable Creative Commons License



https://dspace.org/

Influence of monomer structure and catalyst concentration on topological transition and dynamic properties of dicarboxylic acidepoxy vitrimers

Shen, Shouqi; Thakur, Vijay Kumar; Skordos, Alexandros A.

2024-12-31
Wiley
https://doi.org/10.1002/app.56028
Shen S, Thakur VK, Skordos AA. (2024) Influence of monomer structure and catalyst concentration on topological transition and dynamic properties of dicarboxylic acidepoxy vitrimers. Journal of Applied Polymer Science, Volume 141, Issue 40, October 2024, Article number e56028

Downloaded from a DSpace repository. https://dspace.org/